Wave Motion 51 (2014) 804–817

Contents lists available at ScienceDirect

Wave Motion

journal homepage: www.elsevier.com/locate/wavemoti

Nonlinear interfacial waves in a circular cylindrical container subjected to a vertical excitation

L. Chang [a,b], Y.J. Jian [a,*], J. Su [a], R. Na [a], Q.S. Liu [a], G.W. He [c]

[a] School of Mathematical Science, Inner Mongolia University, Hohhot, Inner Mongolia 010021, China

[b] School of Mathematics and Statistics, Inner Mongolia University of Finance and Economics, Hohhot, Inner Mongolia 010051, China

[c] The State Key Laboratory of Nonlinear Mechanics (LNM), Institute of Mechanics, Chinese Academy of Sciences, Beijing 100080, China

HIGHLIGHTS

- The two-layer ideal fluid interface waves were studied.
- Singular perturbation theory of two-time scale expansions was developed.
- A nonlinear amplitude equation with cubic and vertically excited terms was derived.
- Different surface patterns were obtained for different excited frequencies and amplitudes.

ARTICLE INFO

Article history:
Received 22 May 2013
Received in revised form 21 January 2014
Accepted 1 February 2014
Available online 11 February 2014

Keywords:
Inviscid two-layer fluids
Vertical periodical oscillation
Two-time scale expansions
Nonlinear interfacial waves
Circular cylindrical container

ABSTRACT

Singular perturbation theory of two-time scale expansions was developed in inviscid fluids to investigate the motion of single interface standing wave in a two-layer liquid-filled circular cylindrical vessel, which is subjected to a vertical periodical oscillation. It is assumed that the fluid in the circular cylindrical vessel is inviscid, incompressible and the motion is irrotational, a nonlinear amplitude equation including cubic nonlinear and vertically forced terms, was derived by the method of expansion of two-time scales without taking the influence of surface tension into account. By numerical computation, it is shown that different patterns of interface standing wave can be excited for different driving frequency and amplitude. We found that the interface wave mode become more and more complex as increasing of upper to lower layer density ratio γ. The traits of the standing interface wave were proved theoretically. In addition, the dispersion relation and nonlinear amplitude equation obtained in this article can reduce to the known results for a single fluid when $\gamma = 0$, $h_2 \to h_1$.

1. Introduction

The generation of standing waves at free surface of a liquid subjected to vertical oscillation has already been known since the observations of Faraday [1]. Faraday noted that the fundamental frequency of these surface standing waves equals to one half of the excitation frequency, i.e. the response was subharmonic. Rayleigh [2] also performed this experiment and confirmed the experimental observations of Faraday. Benjamin and Ursell [3] showed that the linear problem can be characterized by Mathieu's equation, which allows harmonic, subharmonic and superharmonic responses. A good overview of the nonlinear effects was given by Miles and Henderson [4].

* Corresponding author. Tel.: +86 471 4991650; fax: +86 471 4991650.
E-mail address: jianyongjun@yahoo.com.cn (Y.J. Jian).

http://dx.doi.org/10.1016/j.wavemoti.2014.02.001
0165-2125/

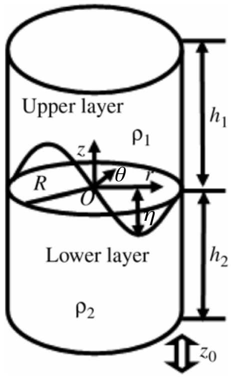

Fig. 1. Physical model of the liquid-filled circular cylindrical vessel, which is subject to a vertical oscillation.

The free surface can be destabilized only in the tongue-like zones in the plane of the forcing amplitude and the selected wave number. The tongues correspond alternately to subharmonic and harmonic responses. For ideal liquids, the lowest points of all these tongues occur for vanishing forcing amplitude a. Therefore, both kinds of responses are possible at the onset.

This classical Faraday wave problem has recently arisen again in two rather different ways. One of these is concerned with the instability [5–11] and chaotic behaviors in the container with a closed basin [12–17]. The other relates to solitary standing waves observed in a long narrow channel [18,19]. More recently, Feng et al. [20] considered surface wave motions in a container with a nearly square base subjected to a vertical oscillation.

Faraday resonance continues to attract the attention of numerous researchers, due in parts to the significance of vertically oscillating flows and to the convenient framework it provides for studies of stability and damping. An example of the former is provided by Foda et al. [21], who studied the Faraday resonance of thin viscoelastic layers. This mechanism was offered as an explanation of the short-scale variability of amplification factors observed in the seismic records of many earthquakes. Kumar [22] also studied the Faraday resonance of waves in viscoelastic fluids, and noted its potential application as a tool for measurement of rheological properties. Of particular interest is the difference in behavior between viscoelastic and Newtonian fluids.

In addition to being ideally suited for experimental studies, the simplicity of the Faraday instability has allowed exploration with several different analytic techniques. For example, straightforward multiple-scales analyses are frequently used in conjunction with solvability conditions in order to obtain an amplitude evolution equation. Miles [23] computed the Lagrangian of the system and then used Hamilton's principle to derive the evolution equation. In addition, Miles [24] discussed a rather compact approach that relied upon specification of the surface-wave "impedance" in order to obtain the threshold forcing required for growth.

Interfacial waves travel along the interface between two fluids with different densities. They can be often observed in subsurface layers of the ocean since the upper subsurface layer is warmer over much of the ocean [25]. They are random and can be excited by many kinds of disturbances from the surface, bottom and interior of a stratified ocean, such as wind stress, the flow over uneven bottoms, the moving body at the surface or under water and the deformations of the seafloor. Over the past decades there have been considerable studies aimed at understanding the generation and the behavior of the surface waves, especially for tsunamis generated by a vertical movement of the ocean floor [26–29]. However, the generation of the internal waves caused by the ocean floor deformations is seldom studied. Due to the similarities between the surface wave and the interfacial wave, it is natural to apply the methods developed for surface waves to the study of interfacial waves as reviewed by Umeyama [30,31]. Using a transform method (Laplace for time and Fourier for space), Song [32] studied the internal and surface waves generated by the deformations of the solid bed in a two layer fluid system of infinite lateral extent. By the method of numerical projection, Louis et al. [33] studied the instability of Faraday wave in the container with irregular bottom. The purpose of this paper is to investigate the Faraday interfacial wave in a circular cylindrical container and to study the dependence of wave patterns on related parameters.

2. Formula deriving and analytical solution

2.1. Governing equations and boundary conditions

We consider interfacial waves excited by the vertical motion of a circular cylindrical basin filled with inviscid fluid, as shown in Fig. 1. We take cylindrical coordinate system (r, θ, z) moving with the vessel, such that the equation of the undisturbed interface is $z = 0$, the base of the vessel is located at $z = -h_2 < 0$, and top of the vessel is located at $z = h_1 > 0$, where $h = h_1 + h_2$ denotes the depth of fluid. If the container is now subjected to a vertical periodic oscillations with the displacement of $z_0 = A\cos(2\omega_0 t)$, where A and $2\omega_0$ are the amplitude and angular frequency of the external forcing, then the fluid moves relatively to the vessel as if it moves at a gravitational acceleration $(g - \ddot{z}_0)$ in a stationary vessel, $\ddot{z}_0$ is the derivative of second order with respect to time t. We can study parametrically excited interface waves within this model. It is assumed that the fluid is incompressible and the motion is irrotational, there must exist velocity potential functions $\phi_j(r, \theta, z, t)$ ($j = 1, 2$ means upper and lower layer fluids, respectively) corresponding to the motions of the upper and the lower fluids, which obey the Laplace equations

$$\frac{\partial^2\phi_1}{\partial r^2} + \frac{1}{r}\frac{\partial\phi_1}{\partial r} + \frac{1}{r^2}\frac{\partial^2\phi_1}{\partial\theta^2} + \frac{\partial^2\phi_1}{\partial z^2} = 0, \quad 0 < r < R,\ \eta(r, \theta, t) \le z \le h_1, \tag{1}$$

$$\frac{\partial^2\phi_2}{\partial r^2} + \frac{1}{r}\frac{\partial\phi_2}{\partial r} + \frac{1}{r^2}\frac{\partial^2\phi_2}{\partial\theta^2} + \frac{\partial^2\phi_2}{\partial z^2} = 0, \quad 0 < r < R,\ -h_2 \le z \le \eta(r, \theta, t). \tag{2}$$

From the Bernoulli equations in each fluid, matching pressures at the interface, we have the following dynamic boundary condition

$$\begin{aligned} &\rho_1\left\{\frac{\partial\phi_1}{\partial t} + \frac{1}{2}\left[\left(\frac{\partial\phi_1}{\partial r}\right)^2 + \frac{1}{r^2}\left(\frac{\partial\phi_1}{\partial\theta}\right)^2 + \left(\frac{\partial\phi_1}{\partial z}\right)^2\right] + (g - \ddot{z}_0)\,\eta\right\} \\ &\quad = \rho_2\left\{\frac{\partial\phi_2}{\partial t} + \frac{1}{2}\left[\left(\frac{\partial\phi_2}{\partial r}\right)^2 + \frac{1}{r^2}\left(\frac{\partial\phi_2}{\partial\theta}\right)^2 + \left(\frac{\partial\phi_2}{\partial z}\right)^2\right] + (g - \ddot{z}_0)\,\eta\right\}, \quad z = \eta(r, \theta, t). \end{aligned} \tag{3}$$

The kinetic boundary conditions at the interface are

$$\frac{\partial\eta}{\partial t} + \frac{1}{r^2}\frac{\partial\phi_j}{\partial\theta}\frac{\partial\eta}{\partial\theta} + \frac{\partial\phi_j}{\partial r}\frac{\partial\eta}{\partial r} - \frac{\partial\phi_j}{\partial z} = 0, \quad z = \eta(r, \theta, t), \tag{4}$$

where $\eta(r, \theta, t)$ is the interface elevation, R is the internal radius of the container, ρ_j denotes the density of the fluid for layer I and layer II, respectively. In addition, since the influence of viscosity is ignored, the boundary conditions at the side walls, top and bottom of the vessel are

$$\frac{\partial\phi_j}{\partial r} = 0, \quad r = R, \tag{5}$$

$$\frac{\partial\phi_j}{\partial z} = 0, \quad z = (-1)^{j+1}h_j, \tag{6}$$

due to zero normal velocity for rigid container. Taking the fluid depth h as the length scale, we introduce the following dimensionless groups

$$\begin{aligned} &z^* = z/h, \quad r^* = r/h, \quad R^* = R/h, \quad h_j^* = h_j/h, \quad A^* = A/h, \quad \eta^* = \eta/h, \\ &t^* = t\sqrt{g/h}, \quad \phi_j^* = \phi_j/(h\sqrt{gh}), \quad \omega_0^* = \omega_0\sqrt{h/g}, \quad \gamma = \rho_1/\rho_2, \quad \varepsilon^2 = 4A\omega_0^2/g, \end{aligned} \tag{7}$$

where γ denotes the density ratio of upper to lower layer, the parameter ε means the acceleration due to the vertical oscillation relative to gravity and is assumed to be much less than unit. The asterisks denote dimensionless quantities and are subsequently dropped. Substituting (7) into (1)–(6), then expanding (3) and (4) into Taylor series at $z = 0$ by neglecting of the term $o(\varepsilon^4)$, nondimensional governing equations and corresponding interfacial conditions can be written as

$$\frac{\partial^2\phi_1}{\partial r^2} + \frac{1}{r}\frac{\partial\phi_1}{\partial r} + \frac{1}{r^2}\frac{\partial^2\phi_1}{\partial\theta^2} + \frac{\partial^2\phi_1}{\partial z^2} = 0, \quad 0 < r < R,\ 0 < z < h_1, \tag{8}$$

$$\frac{\partial^2\phi_2}{\partial r^2} + \frac{1}{r}\frac{\partial\phi_2}{\partial r} + \frac{1}{r^2}\frac{\partial^2\phi_2}{\partial\theta^2} + \frac{\partial^2\phi_2}{\partial z^2} = 0, \quad 0 < r < R,\ -h_2 < z < 0, \tag{9}$$

$$\frac{\partial\eta}{\partial t} - \frac{\partial\phi_j}{\partial z} + \frac{\partial\phi_j}{\partial r}\frac{\partial\eta}{\partial r} + \frac{1}{r^2}\frac{\partial\phi_j}{\partial\theta}\frac{\partial\eta}{\partial\theta} - \frac{\partial^2\phi_j}{\partial z^2}\eta + \frac{\partial^2\phi_j}{\partial r\partial z}\eta\frac{\partial\eta}{\partial r} + \frac{1}{r^2}\frac{\partial^2\phi_j}{\partial\theta\partial z}\eta\frac{\partial\eta}{\partial\theta} - \frac{1}{2}\frac{\partial^3\phi_j}{\partial z^3}\eta^2 = 0, \quad z = 0, \tag{10}$$

$$\begin{aligned} &\frac{\partial\phi_2}{\partial t} + \frac{1}{2}\left[\left(\frac{\partial\phi_2}{\partial r}\right)^2 + \frac{1}{r^2}(\frac{\partial\phi_2}{\partial\theta})^2 + \left(\frac{\partial\phi_2}{\partial z}\right)^2\right] + [1 + f\cos(2\omega_0 t)]\eta + \frac{\partial^2\phi_2}{\partial t\partial z}\eta \\ &\quad + \left(\frac{\partial\phi_2}{\partial r}\frac{\partial^2\phi_2}{\partial r\partial z} + \frac{1}{r^2}\frac{\partial\phi_2}{\partial\theta}\frac{\partial^2\phi_2}{\partial\theta\partial z} + \frac{\partial\phi_2}{\partial z}\frac{\partial^2\phi_2}{\partial z^2}\right)\eta + \frac{1}{2}\frac{\partial^3\phi_2}{\partial t\partial z^2}\eta^2 \\ &= \gamma\left\{\frac{\partial\phi_1}{\partial t} + \frac{1}{2}\left[\left(\frac{\partial\phi_1}{\partial r}\right)^2 + \frac{1}{r^2}(\frac{\partial\phi_1}{\partial\theta})^2 + \left(\frac{\partial\phi_1}{\partial z}\right)^2\right] + [1 + f\cos(2\omega_0 t)]\eta + \frac{\partial^2\phi_1}{\partial t\partial z}\eta\right. \\ &\quad \left. + \left(\frac{\partial\phi_1}{\partial r}\frac{\partial^2\phi_1}{\partial r\partial z} + \frac{1}{r^2}\frac{\partial\phi_1}{\partial\theta}\frac{\partial^2\phi_1}{\partial\theta\partial z} + \frac{\partial\phi_1}{\partial z}\frac{\partial^2\phi_1}{\partial z^2}\right)\eta + \frac{1}{2}\frac{\partial^3\phi_1}{\partial t\partial z^2}\eta^2\right\}, \quad z = 0, \end{aligned} \tag{11}$$

where $f = 4A\omega_0^2$ is second order small quantity of ε, namely, $f = \varepsilon^2 f_0$. In addition, the boundary conditions of ϕ_j at the side walls, top and bottom of the vessel are the same as (5) and (6).

2.2. The solution of the problem and derivation of amplitude equation

In order to use the method of two-time scale perturbation expansion, we introduce a slowly varying time variable τ defined by $\tau = \varepsilon^2 t$. Then we have

$$\partial/\partial t = \partial/\partial t + \varepsilon^2 \partial/\partial\tau + \cdots, \tag{12}$$

here $\partial/\partial t$ denotes the derivative about time t.

The complexity of this problem is that the interfacial elevation is unknown, and must be solved together with velocity potential. We expand the velocity potentials $\phi_j(r, \theta, z, t)$ and interfacial elevation $\eta(r, \theta, t)$ in form of power series

$$\phi_j\,(r, \theta, z, t, \tau) = \varepsilon\phi_j^{(1)} + \varepsilon^2\phi_j^{(2)} + \varepsilon^3\phi_j^{(3)} + \cdots, \tag{13a}$$

$$\eta\,(r, \theta, t, \tau) = \varepsilon\eta_1 + \varepsilon^2\eta_2 + \varepsilon^3\eta_3 + \cdots. \tag{13b}$$

Inserting (12) and (13) into nondimensional equations (8)–(11), we can give each order approximation by comparing the coefficients of the small parameter ε^i at the two sides.

2.2.1. The solutions of the first-order approximation equations

Eliminate η_1 through combining the first order approximate equations (10)–(11), we have

$$\frac{\partial\phi_2^{(1)}}{\partial z} + \frac{\partial^2\phi_2^{(1)}}{\partial t^2} = \gamma\left(\frac{\partial\phi_1^{(1)}}{\partial z} + \frac{\partial^2\phi_1^{(1)}}{\partial t^2}\right), \quad z = 0. \tag{14}$$

Assuming that the solution is symmetric in circumferential direction, one of the solution of $\phi_j^{(1)}$ has the form of $\phi_j^{(1)} = \Phi_j^{(1)}(r, z, \tau)e^{i\Omega t}\cos(m\theta) + C.C.$, here $C.C.$ is a complex conjugate, i is the unit of imaginary number. Substituting $\phi_j^{(1)}$ into first order approximation equations (8)–(9) and (14), we find $\Phi_j^{(1)}(r\,,\, z\,,\, \tau)$ satisfies the following governing equations and interfacial condition

$$\frac{\partial^2\Phi_1^{(1)}}{\partial r^2} + \frac{1}{r}\frac{\partial\Phi_1^{(1)}}{\partial r} - \frac{m^2}{r^2}\Phi_1^{(1)} + \frac{\partial^2\Phi_1^{(1)}}{\partial z^2} = 0, \quad 0 < r < R,\ 0 < z < h_1, \tag{15}$$

$$\frac{\partial^2\Phi_2^{(1)}}{\partial r^2} + \frac{1}{r}\frac{\partial\Phi_2^{(1)}}{\partial r} - \frac{m^2}{r^2}\Phi_2^{(1)} + \frac{\partial^2\Phi_2^{(1)}}{\partial z^2} = 0, \quad 0 < r < R,\ -h_2 < z < 0, \tag{16}$$

$$\frac{\partial\Phi_2^{(1)}}{\partial z} - \Omega^2\Phi_2^{(1)} = \gamma\left[\frac{\partial\Phi_1^{(1)}}{\partial z} - \Omega^2\Phi_1^{(1)}\right], \quad z = 0. \tag{17}$$

Additionally, the boundary conditions of $\Phi_j^{(1)}$ at the side walls, top and bottom of the vessel are the same as (5) and (6). Using separation of variables method, assuming $\Phi_1^{(1)} = A(\tau)R_1(r)Z_1(z)$, $\Phi_2^{(1)} = B(\tau)R_2(r)Z_2(z)$, inserting $\Phi_1^{(1)}$, $\Phi_2^{(1)}$ into Eqs. (15)–(17), we have

$$\phi_1^{(1)} = J_m(\lambda r)\cosh[\lambda(z - h_1)]\left[A(\tau)e^{i\Omega t} + \bar{A}(\tau)e^{-i\Omega t}\right]\cos(m\theta), \tag{18}$$

$$\phi_2^{(1)} = J_m(\lambda r)\cosh[\lambda(z + h_2)][B(\tau)e^{i\Omega t} + \bar{B}(\tau)e^{-i\Omega t}]\cos(m\theta). \tag{19}$$

In addition, we suppose that the η_1 can be expressed as

$$\eta_1 = J_m(\lambda r)\,[C(\tau)e^{i\Omega t} + \bar{C}(\tau)e^{-i\Omega t}]\cos(m\theta), \tag{20}$$

here $\lambda = \lambda_{mn}$ is the nth positive real root of $dJ_m(\lambda_{mn}r)/dr|_{r=R} = 0$, $J_m(r)$ is the mth order Bessel function of first kind, $A(\tau)$, $B(\tau)$, $C(\tau)$ are called the slowly variable complex amplitudes and $\bar{A}(\tau)$, $\bar{B}(\tau)$, $\bar{C}(\tau)$ are their complex conjugates, Ω is the natural frequency of the interface wave. From the first order approximate interfacial condition (10) we found

$$B(\tau) = -\frac{\sinh(\lambda h_1)}{\sinh(\lambda h_2)}A(\tau), \qquad C(\tau) = \frac{i\lambda}{\Omega}\sinh(\lambda h_1)A(\tau). \tag{21}$$

Substituting (18)–(20) into the first order approximate problem, we have

$$MX = 0, \tag{22}$$

where $M = \begin{pmatrix} \lambda\sinh(\lambda h_1) & 0 & i\Omega \\ 0 & -\lambda\sinh(\lambda h_2) & i\Omega \\ i\Omega\gamma\cosh(\lambda h_1) & -i\Omega\cosh(\lambda h_2) & \gamma - 1 \end{pmatrix}$, $X = (A, B, C)^T$.

The dispersion relation can be obtained by setting $\det(M) = 0$, namely

$$\Omega^*(\theta_1 + \gamma\theta_2) + (\gamma - 1)\theta_1\theta_2 = 0, \tag{23}$$

where $\theta_j = \tanh(\lambda h_j)$, $\Omega^* = \Omega^2/\lambda$. When $\gamma = 0$, $h_2 \to h_1$, the dispersion relation reduces to the known result of single layer fluid [6].

2.2.2. The solutions of the second-order approximation equations

Eliminating η_2 by combining the second order approximate equations (10)–(11), substituting (18)–(20) into the second-order problems, and then using (21), the interface conditions which only contain velocity potentials $\phi_j^{(2)}(r, \theta, z, t)$ can be written as

$$\begin{aligned}\frac{\partial^2\phi_2^{(2)}}{\partial t^2} + \frac{\partial\phi_2^{(2)}}{\partial z} - \gamma\left(\frac{\partial^2\phi_1^{(2)}}{\partial t^2} + \frac{\partial\phi_1^{(2)}}{\partial z}\right) &= \{[W_1(r) + W_2(r)\cos(2m\theta)] - \gamma[W_3(r) + W_4(r)\cos(2m\theta)]\} \\ &\quad \times [A^2(\tau)e^{2i\Omega t} - \bar{A}^2(\tau)e^{-2i\Omega t}], \quad z = 0,\end{aligned} \tag{24}$$

$$\frac{\partial\phi_2^{(2)}}{\partial z} - \frac{\partial\phi_1^{(2)}}{\partial z} = [W_5(r) + W_6(r)\cos(2m\theta)][A^2(\tau)e^{2i\Omega t} - \bar{A}^2(\tau)e^{-2i\Omega t}], \quad z = 0. \tag{25}$$

The expressions of $W_1(r)$ to $W_6(r)$ can be found in Appendix A.

From the right hand sides of Eqs. (24) and (25), we can express the second order velocity potentials $\phi_j^{(2)}$ in the following form

$$\phi_j^{(2)} = P_{j,m}(r, z)\cos(2m\theta)[A^2(\tau)e^{2i\Omega t} - \bar{A}^2(\tau)e^{-2i\Omega t}], \tag{26}$$

where $P_{j,m}(r, z)$ is the function of variables r and z. Inserting (26) into the second order problem (8)–(9), and (24)–(25), we find $P_{j,m}(r, z)$ satisfies the following governing equation and interfacial conditions

$$\frac{\partial^2 P_1}{\partial r^2} + \frac{1}{r}\frac{\partial P_1}{\partial r} - \frac{4m^2}{r^2}P_1 + \frac{\partial^2 P_1}{\partial z^2} = 0, \quad 0 < r < R,\ 0 < z < h_1, \tag{27}$$

$$\frac{\partial^2 P_2}{\partial r^2} + \frac{1}{r}\frac{\partial P_2}{\partial r} - \frac{4m^2}{r^2}P_2 + \frac{\partial^2 P_2}{\partial z^2} = 0, \quad 0 < r < R,\ -h_2 < z < 0, \tag{28}$$

$$\left(\frac{\partial P_2}{\partial z} - \frac{\partial P_1}{\partial z}\right)\cos(2m\theta) = W_5(r) + W_6(r)\cos(2m\theta), \quad z = 0, \tag{29}$$

$$\begin{aligned}\left[\left(\frac{\partial P_2}{\partial z} - 4\Omega^2 P_2\right) - \gamma\left(\frac{\partial P_1}{\partial z} - 4\Omega^2 P_1\right)\right]\cos(2m\theta) &= [W_1(r) + W_2(r)\cos(2m\theta)] \\ - \gamma[W_3(r) + W_4(r)\cos(2m\theta)], \quad z = 0.\end{aligned} \tag{30}$$

In addition, the boundary conditions of P_j at the side walls, top and bottom of the vessel are the same as (5) and (6). From (27) and (28), we suppose that $P_{j,m}(r, z)$ satisfies the following Bessel function expansion

$$P_{1,m}(r, z) = \sum_{k=1}^{\infty} d_k \cosh[\lambda_{(2m)k}(z - h_1)]J_{2m}(\lambda_{(2m)k}r), \tag{31}$$

$$P_{2,m}(r, z) = \sum_{k=1}^{\infty} e_k \cosh[\lambda_{(2m)k}(z + h_2)]J_{2m}(\lambda_{(2m)k}r), \tag{32}$$

where $\lambda_{(2m)k}$ denotes the kth root of the derivative of $2m$th order first kind Bessel function, which satisfies the boundary condition $dJ_{2m}(\lambda_{(2m)k}r)/dr|_{r=R} = 0$. The detailed process of determining $P_{j,m}(r, z)$ can be found in Appendix B. On substituting $\phi_j^{(2)}$ into second order dynamic equation at interface, we can obtain the evolution equation for the second order interfacial displacement η_2. For convenience, $\phi_j^{(2)}$ and η_2 can be finally expressed as

$$\phi_1^{(2)} = [X_1(r, z) + X_2(r, z)\cos(2m\theta)][A^2(\tau)e^{2i\Omega t} - \bar{A}^2(\tau)e^{-2i\Omega t}], \tag{33}$$

$$\phi_2^{(2)} = [Y_1(r, z) + Y_2(r, z)\cos(2m\theta)][A^2(\tau)e^{2i\Omega t} - \bar{A}^2(\tau)e^{-2i\Omega t}], \tag{34}$$

$$\eta_2 = [Z_1(r) + Z_2(r)\cos(2m\theta)][A^2(\tau)e^{2i\Omega t} + \bar{A}^2(\tau)e^{-2i\Omega t}] + 2|A(\tau)|^2[S_1(r) + S_2(r)\cos(2m\theta)], \tag{35}$$

where the expressions of $X_j(r, z)$, $Y_j(r, z)$, $Z_j(r)$ and $S_j(r)$ can be found in Appendix C.

So far, we have obtained analytical solutions of the second order velocity potential and interfacial displacement. However, the slowly varying amplitude $A(\tau)$ contained in the solution still cannot be determined. Therefore, it needs to further discuss the third-order problem, and deduce the nonlinear amplitude equation using compatibility condition which must be satisfied by the first-order and the third-order solutions.

2.2.3. Compatibility condition and the derivation of the amplitude equation

Assuming the interfacial wave response is subharmonic, and the interfacial wave frequency is approximately equal to one half of the vertical external forcing frequency, we let

$$\omega_0 - \Omega = \varepsilon^2\sigma, \tag{36}$$

where σ is a constant represents the difference between the interface wave frequency and one half of the drive frequency.

Substituting the first-order solutions (18)–(20) and the second-order solutions (33)–(35) into the third-order problem, we can obtain the third order solution term including factors $\cos(m\theta)\exp(i\Omega t)$ or $\cos(m\theta)\exp(-i\Omega t)$ from interfacial conditions $\frac{\partial\phi_2^{(3)}}{\partial z} - \frac{\partial\phi_1^{(3)}}{\partial z}$ and $\frac{\partial^2\phi_2^{(3)}}{\partial t^2} + \frac{\partial\phi_2^{(3)}}{\partial z} - \gamma[\frac{\partial^2\phi_1^{(3)}}{\partial t^2} + \frac{\partial\phi_1^{(3)}}{\partial z}]$. Assuming the special solution containing factors $\cos(m\theta)\exp(i\Omega t)$ or $\cos(m\theta)\exp(-i\Omega t)$ in the third order problem has the form of $\psi_j^{(3)}(r,z)\cos(m\theta)\exp(i\Omega t)$ or $\psi_j^{(3)}(r,z)\cos(m\theta)\exp(-i\Omega t)$, after complex computation, the $\psi_j^{(3)}(r,z)$ satisfies the following equations

$$\frac{\partial^2\psi_1^{(3)}}{\partial r^2} + \frac{1}{r}\frac{\partial\psi_1^{(3)}}{\partial r} - \frac{m^2}{r^2}\psi_1^{(3)} + \frac{\partial^2\psi_1^{(3)}}{\partial z^2} = 0, \quad 0<r<R,\ 0<z<h_1, \tag{37}$$

$$\frac{\partial^2\psi_2^{(3)}}{\partial r^2} + \frac{1}{r}\frac{\partial\psi_2^{(3)}}{\partial r} - \frac{m^2}{r^2}\psi_2^{(3)} + \frac{\partial^2\psi_2^{(3)}}{\partial z^2} = 0, \quad 0<r<R,\ -h_2<z<0, \tag{38}$$

and interfacial conditions

$$\frac{\partial\psi_2^{(3)}}{\partial z} - \Omega^2\psi_2^{(3)} - \gamma\left[\frac{\partial\psi_1^{(3)}}{\partial z} - \Omega^2\psi_1^{(3)}\right] = E_1(r) - \gamma E_2(r), \quad z=0, \tag{39}$$

$$\frac{\partial\psi_2^{(3)}}{\partial z} - \frac{\partial\psi_1^{(3)}}{\partial z} = E_3(r), \quad z=0, \tag{40}$$

where $E_k(r)$ $(k=1,2,3)$ represents the coefficient containing $\cos(m\theta)\exp(i\Omega t)$ or $\cos(m\theta)\exp(-i\Omega t)$. Additionally, the boundary conditions of $\Psi_j^{(3)}$ at the side walls, top and bottom of the vessel are the same as (5) and (6). $E_1(r) - \gamma E_2(r)$ can be expressed as

$$[G_1(r) - \gamma G_4(r)]A^2(\tau)\bar{A}(\tau) + [G_2(r) - \gamma G_5(r)]\frac{dA(\tau)}{d\tau} + [G_3(r) - \gamma G_3(r)]f_0e^{2i\sigma\tau}\bar{A}(\tau) \tag{41a}$$

or

$$[G_1(r) - \gamma G_4(r)]A(\tau)\bar{A}^2(\tau) - [G_2(r) - \gamma G_5(r)]\frac{d\bar{A}(\tau)}{d\tau} + [G_3(r) - \gamma G_3(r)]f_0e^{2i\sigma\tau}A(\tau), \tag{41b}$$

and $E_3(r)$ is

$$G_7(r)A^2(\tau)\bar{A}(\tau) \tag{41c}$$

or

$$G_7(r)A(\tau)\bar{A}^2(\tau), \tag{41d}$$

where the expressions of $G_1(r)$ to $G_7(r)$ can be found in Appendix D.

Eq. (37) multiplied by $\Phi_1^{(1)}$ subtracts Eq. (15) multiplied by $\Phi_1^{(3)}$, and Eq. (38) multiplied by $\Phi_2^{(1)}$ subtracts Eq. (16) multiplied by $\Phi_2^{(3)}$, then integrating these two equations in the region filled of fluid and using the interfacial conditions (17) and (39)–(40), the third-order problem satisfies the following compatibility condition

$$\int_0^R\left\{[E_1(r) - \gamma E_2(r)]\left(\frac{\theta_1}{\theta_2} + \gamma\right) - \gamma E_3(r)\left(\frac{\theta_1}{\theta_2} + 1\right)\right\}J_m(\lambda r)rdr = 0. \tag{42}$$

The nonlinear amplitude equation (42) can be simplified to

$$i\frac{dA(\tau)}{d\tau} = \frac{\alpha}{\beta}A^2(\tau)\bar{A}(\tau) + \frac{\Gamma}{\beta}e^{2i\sigma\tau}\bar{A}(\tau), \tag{43}$$

where

$$\alpha = \int_0^R J_m(\lambda r) D_1(r) r dr, \qquad \beta = \int_0^R J_m(\lambda r) D_2(r) r dr, \qquad \Gamma = \int_0^R J_m(\lambda r) D_3(r) r dr, \tag{44}$$

and

$$D_1(r) = (G_1(r) - \gamma G_4(r)) \left(\frac{\theta_1}{\theta_2} + \gamma\right) - \gamma G_7(r) \left(\frac{\theta_1}{\theta_2} + 1\right), \tag{45a}$$

$$D_2(r) = (\gamma G_5(r) - G_2(r)) \left(\frac{\theta_1}{\theta_2} + \gamma\right), \tag{45b}$$

$$D_3(r) = (G_3(r) - \gamma G_6(r)) \left(\frac{\theta_1}{\theta_2} + \gamma\right) f_0. \tag{45c}$$

When $\gamma = 0$, $h_2 \to h_1$, the nonlinear amplitude equation (43) reduces to the same result as that of single layer fluid [6], in which interface waves changes with slowly varying time τ. Separating the real and imaginary parts of the unknown function and the coefficients of the amplitude equation (43), one gives the following nonlinear ordinary differential equation groups

$$\frac{dp_1(\tau)}{d\tau} = M_1 p_2(\tau)[p_1^2(\tau) + p_2^2(\tau)] + M_2[p_1(\tau)\sin(2\sigma\tau) - p_2(\tau)\cos(2\sigma\tau)], \tag{46}$$

$$\frac{dp_2(\tau)}{d\tau} = -M_1 p_1(\tau)[p_1^2(\tau) + p_2^2(\tau)] - M_2[p_1(\tau)\cos(2\sigma\tau) + p_2(\tau)\sin(2\sigma\tau)], \tag{47}$$

where

$$M_1 = \frac{\int_0^R J_m(\lambda r) D_1(r) r dr}{\Omega(\frac{\theta_1}{\theta_2} + \gamma)\sinh\lambda h_1 \left[\gamma\left(\frac{\lambda}{\Omega^2} - \frac{1}{\theta_1}\right) - \left(\frac{\lambda}{\Omega^2} + \frac{1}{\theta_2}\right)\right] \int_0^R J_m^2(\lambda r) r dr}, \tag{48a}$$

$$M_2 = \frac{\lambda(\gamma - 1)\left(\frac{1}{2} + \frac{\varepsilon^2\sigma}{\Omega}\right) f_0}{\Omega\left[\gamma\left(\frac{\lambda}{\Omega^2} - \frac{1}{\theta_1}\right) - \left(\frac{\lambda}{\Omega^2} + \frac{1}{\theta_2}\right)\right]}. \tag{48b}$$

The solutions of $p_1(\tau)$ and $p_2(\tau)$ of amplitude equations (46)–(47) can be computed numerically by fourth order Runge–Kutta approach if the appropriate initial conditions are prescribed. Finally, substituting them into the expression of the first-order and second-order velocity potential and interface displacement, we can obtain the solutions of the original equations (1)–(6). In the followings, we will give some results of numerical calculation.

3. Results and discussions

As we know, the small parameter ε is related to forced frequency and amplitude. Thus the forced amplitude must small enough to ensure the validity of small parameter ε in present theory when the forced frequency is given. In order to comparing the results of single layer fluid [7], the contours of the interface displacements and corresponding three dimensional interface figures determined by (13b) for different density ratio γ are plotted in Fig. 2 when the forced frequency is 29.1 Hz and the forced amplitude is 11.4 μm. In Fig. 2 and following related figures, the solid (dashed) lines of the contours represent the position of interface, which is above (blow) the equilibrium interface. In the parametrical couple of (m, n), m stands for the number of the wave-crests in circumferential direction and n is the number of the zero points in radical direction. From Fig. 2 we can easily find that with increasing density ratios, the interface wave patterns become more and more complex due to an increasing wave number from dispersion relation (23).

Fig. 3 illustrates the (9, 6) mode evolution of the interface wave displacement (13b) with non-dimensional variable r ($\theta = 4\pi/3$) and spatial coordinate θ ($r = 0.5$) at different time. It can be seen from Fig. 3 that the positions of nodes are constant and only the amplitude changes up and down, which explains the property of the standing interface wave.

The three-dimensional interface displacement of (9, 6) mode at different time can be seen in Fig. 4. When $t = 0.09$ s in Fig. 4(a), the displacement of interface wave in the point of S obtains its positive maximum, where the point S denotes the interface wave in this specific position at this time. As showed in Fig. 4(b), the displacement of location S decreases with the development of time. It can be seen from in Fig. 4(c) that the displacement of the interface wave in S location changes from above equilibrium to below it and the displacement becomes negative in next time $t = 0.5399$ s. Fig. 4(d) shows that the displacement in S location becomes the negative maximum with the evolution of time. Besides, the displacement of S will decrease and then obtain its positive maximum with the development of time. The trait of standing interface wave is proved theoretically.

It is necessary to point out that the location S is only a typical interface wave location, and other displaces still have the same characters as the point S. For interface wave, moreover, (9, 6) mode is a special case, and by the same approach, we can study other modes of the interface waves.

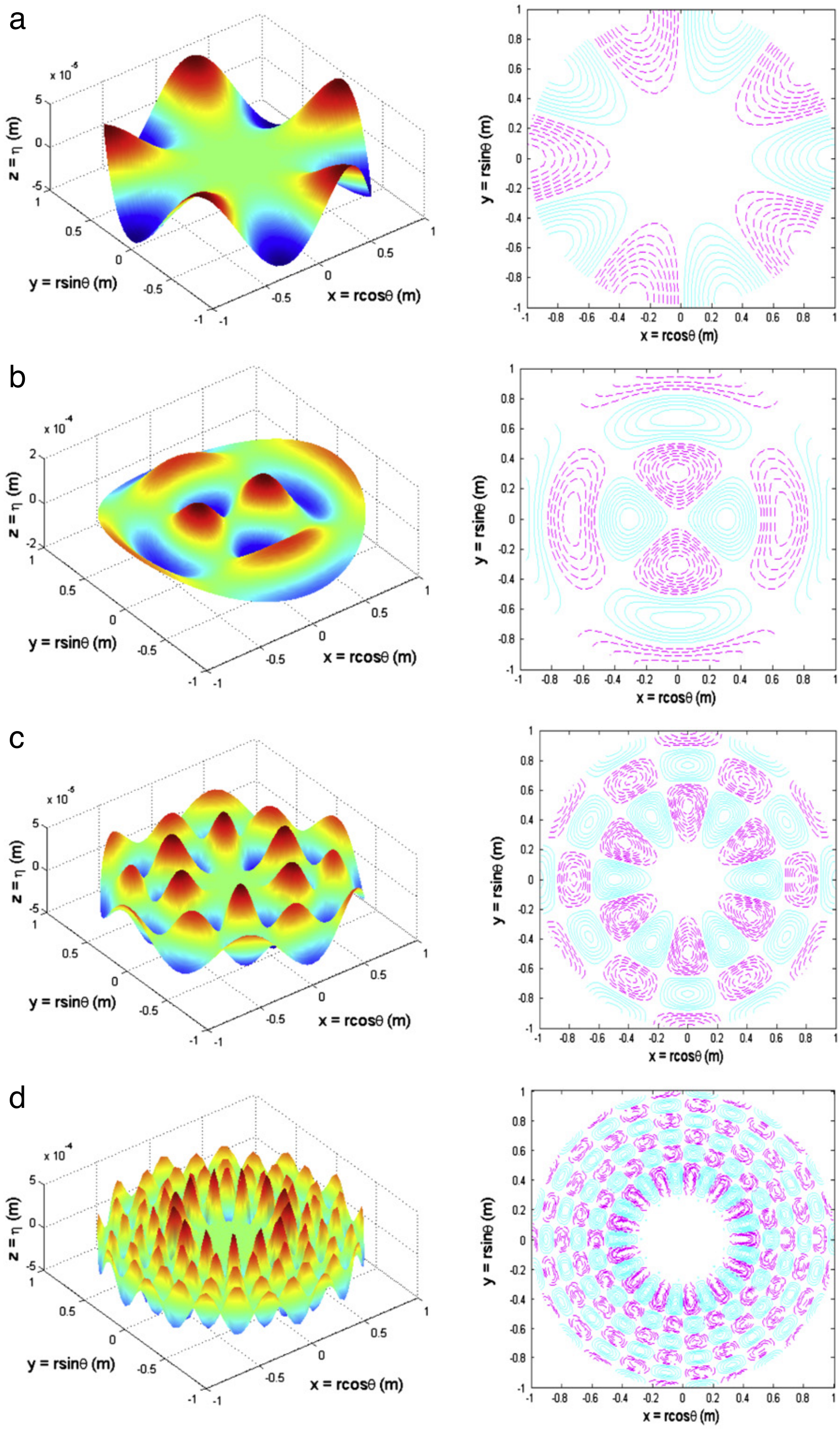

Fig. 2. Contours (right) and three-dimensional modes (left) of the interface wave at different density ratio γ (depth of fluid $h_1 = h_2 = 5$ mm, radius of vessel is $R = 7.5$ cm, forcing amplitude $A = 11.4$ μm, forced frequencies $f = 29.1$ Hz) (a) $\gamma = 0.0$, (5, 1) mode; (b) $\gamma = 0.3$, (2, 3) mode; (c) $\gamma = 0.8$, (6, 3) mode; (d) $\gamma = 0.9$, (13, 6) mode.

As shown in Fig. 5(a) and (c), the interface wave modes of (3, 2) and (13, 6) oscillate at first. With the evolution of the time, a stable periodical solution can be formed. Similarly, Fig. 5(b) and (d) indicate that the interface wave tends to a stable forced oscillation with the evolution of time.

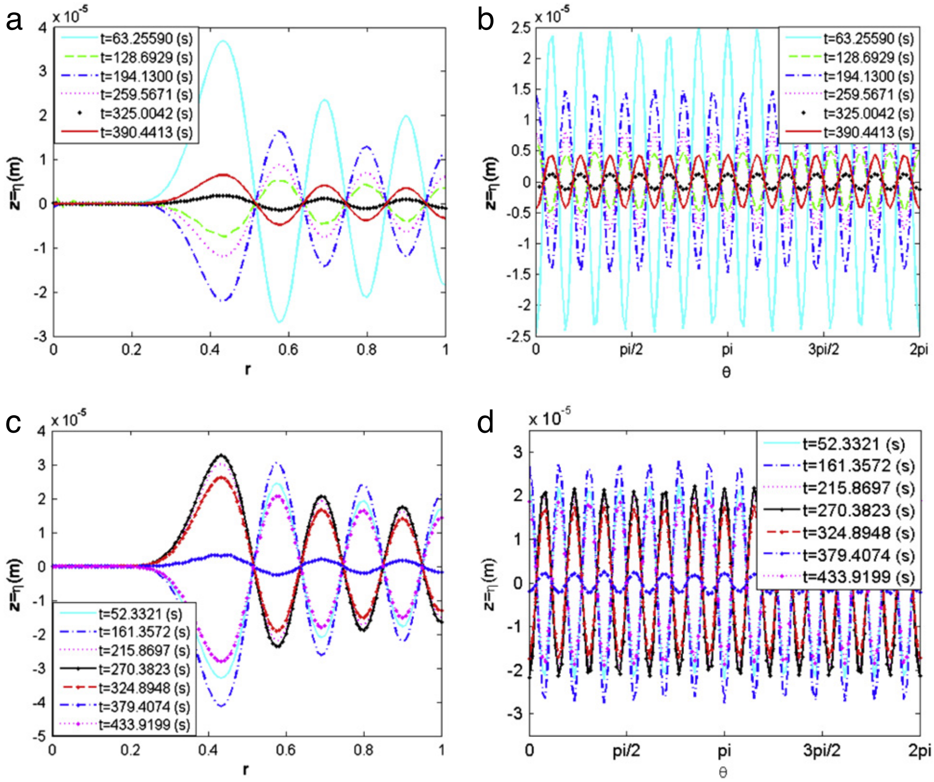

Fig. 3. Spatial evolution of interface wave displacement of (9, 6) mode with radius r and azimuth θ at different time (density of fluid $\rho_1 = 415.667$ kg m^3, $\rho_2 = 519.933$ kg m^{-3}, radius of the vessel $R = 7.5$ cm, forced frequency $f = 20.9$ Hz, forced amplitude $A = 11.4$ μm) (a) Interfacial variations with radius $r(\theta = 4\pi/3, h_1 = 5$ mm, $h_2 = 7$ mm); (b) Interfacial variations with azimuth θ ($r = 0.5$, $h_1 = 5$ mm, $h_2 = 7$ mm); (c) Interfacial variations with radius $r(\theta = 4\pi/3, h_1 = h_2 = 5$ mm); (d) Interfacial variation with azimuth θ ($r = 0.5$, $h_1 = h_2 = 5$ mm).

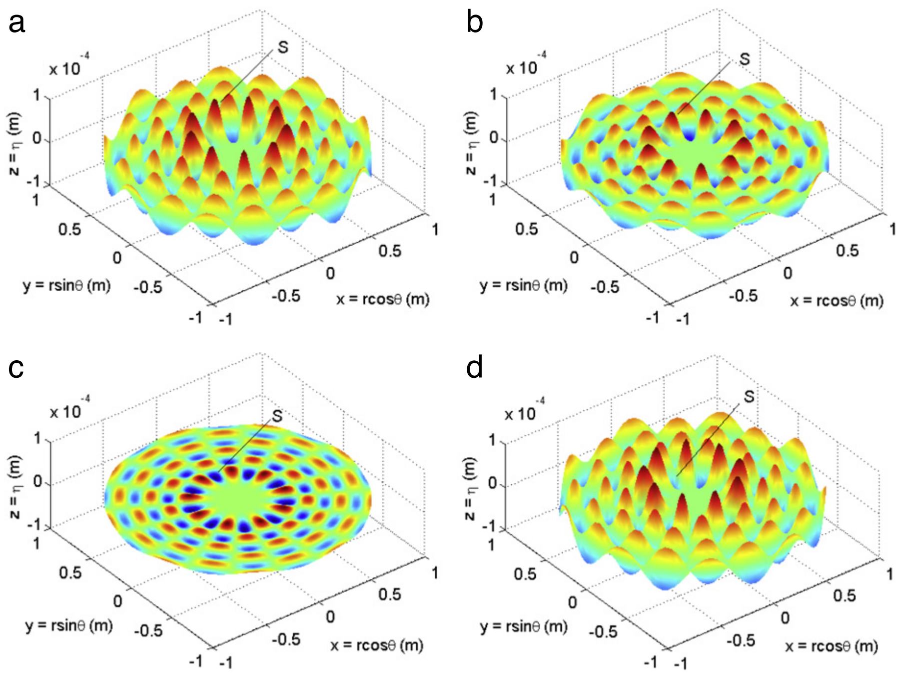

Fig. 4. Three-dimensional interfacial displacement of (9, 6) mode at different time t (density ratios $\gamma = 0.5$, depth of fluid $h_1 = h_2 = 5$ mm, radius of the vessel $R = 7.5$ cm, forced frequency $f = 29.1$ Hz, forced amplitude $A = 11.4$ μm) (a) $t = 0.0900$ s; (b) $t = 0.3149$ s; (c) $t = 0.5399$ s; (d) $t = 1.0798$ s.

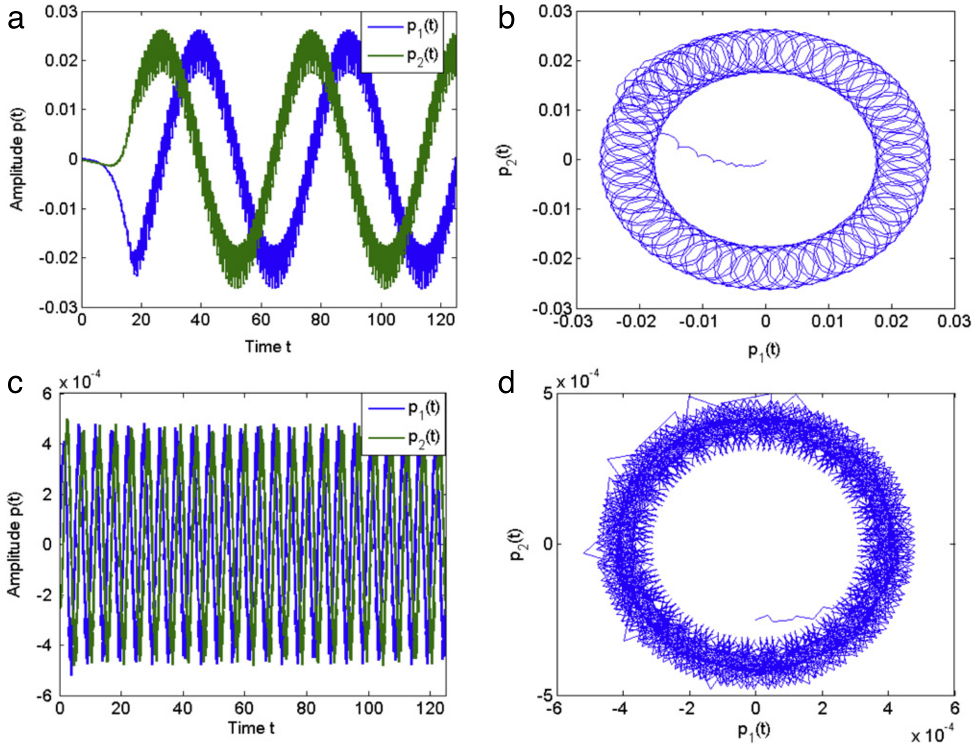

Fig. 5. The evolution of the amplitude $p(\tau)$ with time and phase-plane trajectory ($R = 7.5$ cm, $h_1 = h_2 = 5$ mm, $A = 11.4$ μm) (a) The evolution of the amplitude $p(\tau)$ with time ($\gamma = 0.3, f = 29.1$ Hz, (3, 2) mode); (b) the phase-plane trajectory of $p_1(\tau)$ and $p_2(\tau)$ ($\gamma = 0.3, f = 29.1$ Hz, (3, 2) mode); (c) The evolution of the amplitude $p(\tau)$ with time($\gamma = 0.9, f = 50$ Hz, (13,6) mode); (d) the phase-plane trajectory of $p_1(\tau)$ and $p_2(\tau)$ ($\gamma = 0.9, f = 50$ Hz, (13,6) mode).

4. Concluding remarks

In the inviscid fluids, the vertically excited interface waves in a circular cylindrical vessel are studied by two-time scale perturbation expansions. We found the following results:

(i) We derived a nonlinear evolution equation of slowly varying amplitude with the influence of cubic nonlinearity and external excitation, which expands the results of single layer fluid.
(ii) The interface wave modes become more and more complex with the increase of the density ratio of upper to lower fluids.
(iii) The trait of standing interface wave is proved theoretically.
(iv) When $\gamma = 0$, $h_2 \to h_1$, the dispersion relation and nonlinear amplitude equation reduces to the known results of single layer fluid.

Acknowledgments

The work was supported by the National Natural Science Foundation of China (Grant Nos. 11062005, 11202092, 11362012), Opening fund of State Key Laboratory of Nonlinear Mechanics, the Program for Young Talents of Science and Technology in Universities of Inner Mongolia Autonomous Region (Grant No. NJYT-13-A02), the Natural Science Foundation of Inner Mongolia (Grant Nos. 2010BS0107, 2012MS0107), Research Program of Science and Technology at Universities of Inner Mongolia Autonomous Region, the postgraduate scientific research innovation project of Inner Mongolia and the enhancing comprehensive strength project of Inner Mongolia University (Grant No. 1402020201).

Appendix A

$$W_1(r) = W_2(r) - \frac{i\lambda m^2 \sinh^2(\lambda h_1)}{r^2\theta_2}\left(\frac{1}{\Omega} + \frac{\Omega}{\lambda\theta_2}\right)J_m^2(\lambda r), \tag{A.1}$$

$$\begin{aligned} W_2(r) \;=\; & \frac{i\lambda^2 \sinh^2(\lambda h_1)}{2}\left(\frac{\lambda}{\Omega\theta_2} - 2\Omega\right)J_m^2(\lambda r) + \frac{i\lambda^2 \sinh^2(\lambda h_1)}{\theta_2}\left(\frac{1}{\Omega} + \frac{\Omega}{\lambda\theta_2}\right)J_{m+1}(\lambda r) \\ & \times \left[\frac{m}{r}J_m(\lambda r) - \frac{\lambda}{2}J_{m+1}(\lambda r)\right], \end{aligned} \tag{A.2}$$

$$W_3(r) = W_4(r) + \frac{im^2\cosh^2(\lambda h_1)}{r^2}\left(\frac{\lambda\theta_1}{\Omega} - \Omega\right)J_m^2(\lambda r), \tag{A.3}$$

$$\begin{aligned} W_4(r) &= \frac{i\lambda^2\theta_1 \cos h^2(\lambda h_1)}{2}\left[(1-3i\Omega)\theta_1 - \frac{\lambda}{\Omega}\right]J_m^2(\lambda r) - i\lambda\cosh^2(\lambda h_1)\left(\frac{\lambda\theta_1}{\Omega} - \Omega\right)J_{m+1}(\lambda r) \\ &\quad \times \left[\frac{m}{r}J_m(\lambda r) - \frac{\lambda}{2}J_{m+1}(\lambda r)\right], \end{aligned} \tag{A.4}$$

$$W_5(r) = W_6(r) - \frac{i\lambda m^2 \sinh(2\lambda h_1)}{2r^2\Omega}\left(\frac{\theta_1}{\theta_2} + 1\right)J_m^2(\lambda r), \tag{A.5}$$

$$W_6(r) = \frac{i\lambda^3\sinh^2(\lambda h_1)}{2\Omega}\left(\frac{1}{\theta_2} + \frac{1}{\theta_1}\right)J_m^2(\lambda r) + \frac{i\lambda^2\sinh^2(2\lambda h_1)}{2\Omega}\left(\frac{\theta_1}{\theta_2} + 1\right)J_{m+1}(\lambda r)\left[\frac{m}{r}J_m(\lambda r) - \frac{\lambda}{2}J_{m+1}(\lambda r)\right]. \tag{A.6}$$

Appendix B

Substituting (31), (32) into (29), (30), we have

$$\begin{aligned} &\sum_{k=1}^{\infty}\{e_k\lambda_{(2m)k}\sinh[\lambda_{(2m)k}h_2] + d_k\lambda_{(2m)k}\sinh[\lambda_{(2m)k}h_1]\}J_{2m}(\lambda_{(2m)k}r)\cos(2m\theta) \\ &\quad = W_5(r) + W_6(r)\cos(2m\theta), \quad z = 0, \end{aligned} \tag{B.1}$$

$$\begin{aligned} &\sum_{k=1}^{\infty}\{e_k\cosh[\lambda_{(2m)k}h_2][\lambda_{(2m)k}\tanh[\lambda_{(2m)k}h_2] - 4\Omega^2] + \gamma d_k\cosh[\lambda_{(2m)k}h_1][\lambda_{(2m)k}\tanh[\lambda_{(2m)k}h_1] + 4\Omega^2]\} \\ &\quad \times J_{2m}(\lambda_{(2m)k}r)\cos(2m\theta) = [W_1(r) - \gamma W_3(r)] + [W_2(r) - \gamma W_4(r)]\cos(2m\theta), \quad z = 0. \end{aligned} \tag{B.2}$$

Using the orthogonality of the Bessel function, the coefficients d_k and e_k can be expressed. The final analytical expressions of the second-order solution $\phi_j^{(2)}$ can be written as

$$\phi_j^{(2)} = [P_{j,0}(r,z) + P_{j,m}(r,z)\cos(2m\theta)][A^2(\tau)e^{2i\Omega t} - \bar{A}^2(\tau)e^{-2i\Omega t}], \tag{B.3}$$

where

$$P_{1,0}(r,z) = \sum_{k=1}^{\infty} d_{k,0}\cosh[\lambda_{(0)k}(z-h_1)]J_0(\lambda_{(0)k}r), \tag{B.4}$$

$$\begin{aligned} d_{k,0} &= \left\{\lambda_{(0)k}\sinh(\lambda_{(0)k}h_2)\int_0^R [W_1(r) - \gamma W_3(r)]J_0(\lambda_{(0)k}r)rdr - \Delta_{(0)k}^{(2)}\cosh(\lambda_{(0)k}h_2)\right. \\ &\quad \left.\times \int_0^R W_5(r)J_0(\lambda_{(0)k}r)rdr\right\} \Big/ \{N_{(0)k}\lambda_{(0)k}[\gamma\Delta_{(0)k}^{(1)}\sinh(\lambda_{(0)k}h_2)\cosh(\lambda_{(0)k}h_1) \\ &\quad - \Delta_{(0)k}^{(2)}\sinh(\lambda_{(0)k}h_1)\cosh(\lambda_{(0)k}h_2)]\}, \end{aligned} \tag{B.5}$$

$$P_{1,m}(r,z) = \sum_{k=1}^{\infty} d_{k,m}\cosh[\lambda_{(2m)k}(z-h_1)]J_{2m}(\lambda_{(2m)k}r), \tag{B.6}$$

$$\begin{aligned} d_{k,m} &= \left\{\lambda_{(2m)k}\sinh(\lambda_{(2m)k}h_2)\int_0^R [W_2(r) - \gamma W_4(r)]J_{2m}(\lambda_{(2m)k}r)rdr - \Delta_{(2m)k}^{(2)}\cosh(\lambda_{(2m)k}h_2)\right. \\ &\quad \left.\times \int_0^R W_6(r)J_{2m}(\lambda_{(2m)k}r)rdr\right\} \Big/ \{N_{(2m)k}\lambda_{(2m)k}[\gamma\Delta_{(2m)k}^{(1)}\sinh(\lambda_{(2m)k}h_2)\cosh(\lambda_{(2m)k}h_1) \\ &\quad - \Delta_{(2m)k}^{(2)}\sinh(\lambda_{(2m)k}h_1)\cosh(\lambda_{(2m)k}h_2)]\}, \end{aligned} \tag{B.7}$$

$$P_{2,0}(r,z) = \sum_{k=1}^{\infty} e_{k,0}\cosh[\lambda_{(0)k}(z+h_2)]J_0(\lambda_{(0)k}r), \tag{B.8}$$

$$\begin{aligned} e_{k,0} &= \left\{\lambda_{(0)k}\sinh(\lambda_{(0)k}h_1)\int_0^R [W_1(r) - \gamma W_3(r)]J_0(\lambda_{(0)k}r)rdr - \gamma\Delta_{(0)k}^{(1)}\cosh(\lambda_{(0)k}h_1)\right. \\ &\quad \left.\times \int_0^R W_5(r)J_0(\lambda_{(0)k}r)rdr\right\} \Big/ \{N_{(0)k}\lambda_{(0)k}[\Delta_{(0)k}^{(2)}\sinh(\lambda_{(0)k}h_1)\cosh(\lambda_{(0)k}h_2) \\ &\quad - \gamma\sinh(\lambda_{(0)k}h_2)\cosh(\lambda_{(0)k}h_1)]\}, \end{aligned} \tag{B.9}$$

$$P_{2,m}(r,z)=\sum_{k=1}^{\infty}e_{k,m}\cosh[\lambda_{(2m)k}(z+h_2)]J_{2m}(\lambda_{(2m)k}r), \tag{B.10}$$

$$\begin{aligned}e_{k,m} \ = \ & \left\{\lambda_{(2m)k}\sinh(\lambda_{(2m)k}h_1)\int_0^R[W_1(r)-\gamma W_3(r)]J_{2m}(\lambda_{(2m)k}r)rdr-\gamma\Delta^{(1)}_{(2m)k}\cosh(\lambda_{(2m)k}h_1)\right.\\ & \left.\times\int_0^R W_5(r)J_{2m}(\lambda_{(2m)k}r)rdr\right\}\Big/\{N_{(2m)k}\lambda_{(2m)k}[\Delta^{(2)}_{(2m)k}\sinh(\lambda_{(2m)k}h_1)\cosh(\lambda_{(2m)k}h_2)\\ & -\gamma\sinh(\lambda_{(2m)k}h_2)\cosh(\lambda_{(2m)k}h_1)]\},\end{aligned} \tag{B.11}$$

where $\Delta^{(2)}_{(2m)k}=\lambda_{(2m)k}\tanh(\lambda_{(2m)k}h_2)-4\Omega^2$, $\Delta^{(1)}_{(2m)k}=\lambda_{(2m)k}\tanh(\lambda_{(2m)k}h_1)+4\Omega^2$,

$$N_{(2m)k}=\int_0^R rJ^2_{2m}(\lambda_{(2m)k}r)dr=\frac{(R^2\lambda^2_{(2m)k}-4m^2)J^2_{2m}(\lambda_{(2m)k}R)}{2\lambda^2_{(2m)k}}. \tag{B.12}$$

Appendix C

$$\begin{aligned}&X_1(r,z)=P_{1,0}(r,z),\qquad X_2(r,z)=P_{1,m}(r,z),\qquad Y_1(r,z)=P_{2,0}(r,z),\qquad Y_2(r,z)=P_{2,m}(r,z),\\ &Z_1(r)=K_1(r)+K_2(r)+K_3(r)+\frac{2i\Omega}{1-\gamma}(\gamma P_{1,0}-P_{2,0}),\qquad Z_2(r)=K_1(r)+K_3(r)+\frac{2i\Omega}{1-\gamma}(\gamma P_{1,m}-P_{2,m}),\\ &S_1(r)=-K_1(r)+K_2(r)+K_3(r),S_2(r)=-K_1(r)+K_3(r),\end{aligned} \tag{C.1}$$

where

$$\begin{aligned}&K_1(r)=\frac{\lambda^2(2\gamma-3)}{4(1-\gamma)}\sinh^2(\lambda h_1)J^2_m(\lambda r),\qquad K_2(r)=\frac{m^2\cosh^2(\lambda h_1)}{2r^2(1-\gamma)}\left(\gamma-\frac{\theta_1^2}{\theta_2^2}\right)J^2_m(\lambda r),\\ &K_3(r)=\frac{\lambda\cosh^2(\lambda h_1)}{2(1-\gamma)}\left(\gamma-\frac{\theta_1^2}{\theta_2^2}\right)J_{m+1}(\lambda r)\left[\frac{\lambda}{2}J_{m+1}(\lambda r)-\frac{m}{r}J_m(\lambda r)\right].\end{aligned} \tag{C.2}$$

Appendix D

$$\begin{aligned}G_1(r)\ =\ & \lambda^2\sinh^3(\lambda h_1)\left(\frac{1}{\theta_2}-\frac{\lambda}{\Omega^2}\right)J_m(\lambda r)\left[-\lambda J_{m+1}(\lambda r)+\frac{m}{r}J_m(\lambda r)\right]^2+\lambda^2\sinh^3(\lambda h_1)\left[\frac{\lambda^2}{2}\left(\lambda-\frac{1}{\theta_2}\right)\right.\\ & \left.+\ \frac{m^2}{r^2}\left(1-\frac{\lambda}{\Omega^2}\right)\right]J^3_m(\lambda r)+\sinh(\lambda h_1)\left[i\Omega\left(\frac{1}{\theta_2}-\frac{\lambda}{\Omega^2}\right)\left(\frac{\partial Y_1(r,z)}{\partial r}\Big|_{z=0}+\frac{1}{2}\frac{\partial Y_2(r,z)}{\partial r}\Big|_{z=0}\right)\right.\\ & \left.-\ \frac{1}{\theta_2}\left(Z_1'(r)+\frac{1}{2}Z_2'(r)+2S_1'(r)+S_2'(r)\right)\right]\left[-\lambda J_{m+1}(\lambda r)+\frac{m}{r}J_m(\lambda r)\right]\\ & +i\Omega\lambda\sinh(\lambda h_1)\left[\frac{\partial Y_1(r,z)}{\partial z}|_{z=0}+\frac{1}{2}\frac{\partial Y_2(r,z)}{\partial z}|_{z=0}\right.\\ & \left.+\ \frac{1}{\Omega^2}\left(\frac{\partial^2Y_1(r,z)}{\partial z^2}|_{z=0}+\frac{1}{2}\frac{\partial^2Y_2(r,z)}{\partial z^2}|_{z=0}\right)\right]J_m(\lambda r)\\ & +\frac{m^2\sinh(\lambda h_1)}{r^2\theta_2}[i\Omega Y_2(r,0)-Z_2(r)-2S_2(r)]J_m(\lambda r)-\frac{i\lambda m^2\sinh(\lambda h_1)}{r^2\Omega}Y_2(r,0)J_m(\lambda r)\\ & +\frac{\lambda^2\sinh(\lambda h_1)}{\theta_2}\left[Z_1(r)+\frac{1}{2}Z_2(r)+2S_1(r)+S_2(r)\right]J_m(\lambda r),\end{aligned} \tag{D.1}$$

$$G_2(r)\ =\ \Omega\sinh(\lambda h_1)\left(\frac{\lambda}{\Omega^2}+\frac{1}{\theta_2}\right)J_m(\lambda r), \tag{D.2}$$

$$G_3(r)\ =\ -\lambda\sinh(\lambda h_1)\left(0.5+\frac{\varepsilon^2\sigma}{\Omega}\right)J_m(\lambda r), \tag{D.3}$$

$$
\begin{aligned}
G_4(r) = & -\lambda^2 \sinh^2(\lambda h_1)\cosh(\lambda h_1)\left(1+\frac{\lambda}{\Omega^2}\theta_1\right)J_m(\lambda r)\left[-\lambda J_{m+1}(\lambda r)+\frac{m}{r}J_m(\lambda r)\right]^2 \\
& +\lambda^2 \sinh^2(\lambda h_1)\cosh(\lambda h_1)\left(1+\frac{\lambda}{\Omega^2}\theta_1\right)\left(\frac{\lambda^2}{2}-\frac{m^2}{r^2}\right)J_m^3(\lambda r)+\cosh(\lambda h_1)\left[Z_1'(r)+\frac{1}{2}Z_2'(r)+2S_1'(r)\right. \\
& \left.+\ S_2'(r)-i\Omega\left(1+\frac{\lambda}{\Omega^2}\theta_1\right)\left(\left.\frac{\partial X_1(r,z)}{\partial r}\right|_{z=0}+\frac{1}{2}\left.\frac{\partial X_2(r,z)}{\partial r}\right|_{z=0}\right)\right]\left[-\lambda J_{m+1}(\lambda r)+\frac{m}{r}J_m(\lambda r)\right] \\
& +i\Omega\lambda\sinh(\lambda h_1)\left[\frac{1}{\Omega^2}\left(\left.\frac{\partial^2 X_1(r,z)}{\partial z^2}\right|_{z=0}+\frac{1}{2}\left.\frac{\partial^2 X_2(r,z)}{\partial z^2}\right|_{z=0}\right)-\frac{\partial X_1(r,z)}{\partial z}|_{z=0}-\frac{1}{2}\frac{\partial X_2(r,z)}{\partial z}|_{z=0}\right]J_m(\lambda r) \\
& +\frac{m^2\cosh(\lambda h_1)}{r^2}[Z_2(r)+2S_2(r)-i\Omega X_2(r,0)]J_m(\lambda r)-\frac{i\lambda m^2\sinh(\lambda h_1)}{r^2\Omega}X_2(r,0)J_m(\lambda r) \\
& +\lambda^2\cosh(\lambda h_1)\left[\left(\frac{\Omega^2}{\lambda}\theta_1-1\right)\left(Z_1(r)+\frac{1}{2}Z_2(r)\right)-2\left(\frac{\Omega^2}{\lambda}\theta_1+1\right)\left(S_1(r)+\frac{1}{2}S_2(r)\right)\right]J_m(\lambda r),
\end{aligned} \tag{D.4}
$$

$$
G_5(r) = \Omega\cosh(\lambda h_1)\left(\frac{\lambda}{\Omega^2}\theta_1-1\right)J_m(\lambda r), \tag{D.5}
$$

$$
G_6(r) = -\lambda\sinh(\lambda h_1)\left(0.5+\frac{\varepsilon^2\sigma}{\Omega}\right)J_m(\lambda r), \tag{D.6}
$$

$$
\begin{aligned}
G_7(r) = & \left(1+\frac{\theta_1}{\theta_2}\right)\cosh(\lambda h_1)\left[\lambda J_{m+1}(\lambda r)-\frac{m}{r}J_m(\lambda r)\right]\left[Z_1'(r)+\frac{1}{2}Z_2'(r)+2S_1'(r)+S_2'(r)\right] \\
& +\frac{i\lambda\sinh(\lambda h_1)}{\Omega}\left[\lambda J_{m+1}(\lambda r)-\frac{m}{r}J_m(\lambda r)\right]\left[\left.\frac{\partial Y_1(r,z)}{\partial r}\right|_{z=0}\right. \\
& \left.+\ \frac{1}{2}\left.\frac{\partial Y_2(r,z)}{\partial r}\right|_{z=0}-\left.\frac{\partial X_1(r,z)}{\partial r}\right|_{z=0}-\frac{1}{2}\left.\frac{\partial X_2(r,z)}{\partial r}\right|_{z=0}\right] \\
& -\frac{m^2\cosh(\lambda h_1)}{r^2}\left(1+\frac{\theta_1}{\theta_2}\right)J_m(\lambda r)[Z_2(r)+2S_2(r)]-\frac{i\lambda m^2\sinh(\lambda h_1)}{r^2\Omega}[Y_2(r,0) \\
& -X_2(r,0)]J_m(\lambda r)+\left(1+\frac{\theta_1}{\theta_2}\right)\lambda^2\cosh(\lambda h_1)\left[Z_1(r)+\frac{1}{2}Z_2(r)+2S_1(r)+S_2(r)\right]J_m(\lambda r)+\frac{i\lambda\sinh(\lambda h_1)}{\Omega} \\
& \times J_m(\lambda r)\left(\left.\frac{\partial^2 Y_1(r,z)}{\partial z^2}\right|_{z=0}+\frac{1}{2}\left.\frac{\partial^2 Y_2(r,z)}{\partial z^2}\right|_{z=0}-\left.\frac{\partial^2 X_1(r,z)}{\partial z^2}\right|_{z=0}-\frac{1}{2}\left.\frac{\partial^2 X_2(r,z)}{\partial z^2}\right|_{z=0}\right).
\end{aligned} \tag{D.7}
$$

References

[1] M. Faraday, On the forms and states assumed by fluids in contact with vibrating elastic surfaces, Phil. Trans. R. Soc. London 52 (1831) 319–340.
[2] L. Rayleigh, On the crispations of fluid resting upon a vibrating support, Phil. Mag. 16 (1883) 50–58.
[3] T.B. Benjamin, F. Ursell, The stability of the plane free surface of a liquid in vertical periodic motion, Proc. R. Soc. Lond. A. 225 (1954) 505–515.
[4] J.W. Miles, D. Henderson, Parametrically forced surface waves, Annu. Rev. Fluid Dyn. 22 (1990) 143–165.
[5] J.W. Miles, Parametrically excited solitary waves, J. Fluid Mech. 148 (1984) 451–460.
[6] Y.J. Jian, X.Q. E, W. Bai, Nonlinear Faraday waves in a parametrically excited circular cylindrical container, Appl. Math. Mech. (English Edition) 24 (2003) 1194–1207.
[7] Y.J. Jian, X.Q. E, Instability analysis of nonlinear surface waves in a circular cylindrical container subjected to a vertical excitation, European J. Mech. B/Fluids 24 (2005) 683–702.
[8] Y.J. Jian, X.Q. E, J. Zhang, J.M. Meng, Effect of surface tension on the mode selection of vertically excited surface waves in a circular cylindrical vessel, Chin. Phys. B 13 (2004) 2013–2020.
[9] Y.J. Jian, X.Q. E, J. Zhang, J.M. Meng, Surface waves in a vertically excited circular cylindrical container, Chin. Phys. B 13 (2004) 1623–1630.
[10] Y.J. Jian, X.Q. E, Instability of the vertically forced surface wave in a circular cylindrical container, Chin. Phys. B 13 (2004) 1631–1638.
[11] Y.J. Jian, X.Q. E, Vertically forced surface wave in weakly viscous fluids bounded in a circular cylindrical vessel, Chin. Phys. B 13 (2004) 1191–1200.
[12] R. Keolian, L.A. Turkevich, S.J. Putterman, I. Rudnick, J.A. Rudnick, Subharmonic sequences in the Faraday experiment: departures from period doubling, Phys. Rev. Lett. 47 (1981) 1133–1136.
[13] J.P. Gollub, C.W. Meyer, Symmetry-breaking instabilities on a fluid surface, Phys. D: 6 (1983) 337–346.
[14] S. Ciliberto, J.P. Gollub, Pattern competition leads to chaos, Phys. Rev. Lett. 52 (1984) 922–925.
[15] S. Ciliberto, J.P. Gollub, Chaotic mode competition in parametrically forced surface waves, J. Fluid Mech. 158 (1985) 381–398.
[16] P.J. Holmes, Chaotic motions in a weakly nonlinear model for surface waves, J. Fluid Mech. 162 (1986) 365–388.
[17] F. Simonelli, J.P. Gollub, Surface wave mode interactions: effects of symmetry and degeneracy, J. Fluid Mech. 199 (1989) 471–494.
[18] J. Wu, R. Keolian, I. Rudnick, Observation of a non-propagating hydrodynamic soliton, Phys. Rev. Lett. 52 (1984) 1421–1424.

[19] A. Larraza, S. Putterman, Theory of non-propagating surface-wave solitons, J. Fluid Mech. 148 (1984) 443–449.
[20] Z.C. Feng, P.R. Sethna, Symmetry-breaking bifurcations in resonant surface waves, J. Fluid Mech. 199 (1989) 495–518.
[21] M.A. Foda, S.Y. Tzang, Resonant fluidization of silty soil by water waves, J. Geophys. Res. [Oceans] 99 (1994) 20463.
[22] S. Kumar, Parametrically driven surface waves in viscoelastic liquids, Phys. Fluids 11 (1999) 1970–1981.
[23] J.W. Miles, Nonlinear Faraday resonance, J. Fluid Mech. 146 (1984) 285–302.
[24] J. Miles, On Faraday resonance of a viscous fluid, J. Fluid Mech. 395 (1999) 321–325.
[25] M. Umeyama, Experimental and theoretical analyses of internal waves of finite amplitude, J. Waterway Port Coastal Ocean Eng. 128 (2002) 133–141.
[26] D. Dutykh, F. Dias, Water waves generated by a moving bottom, in: A. Kundu (Ed.), Tsunami and Nonlinear Waves, Springer, Heidelberg, 2007, Geo Sc..
[27] J.L. Hammack, A note on tsunamis: their generation and propagation in an ocean of uniform depth, J. Fluid Mech. 60 (1973) 769–799.
[28] J.M. Johnson, Heterogeneous coupling along Alaska-Aleutians and interred from tsunami, seismic, and geodetic inversions, Adv. Geophys. 39 (1999) 1–116.
[29] Y. Kervella, D. Dutykh, F. Dias, Comparison between three-dimensional linear and nonlinear tsunami generation models, Theor. Comput. Fluid Dyn. 21 (2007) 245–269.
[30] M. Umeyama, Second-order interfacial wave theory by a perturbation method, Mem. Tokyo Met. Univ. 48 (1998) 137–145.
[31] M. Umeyama, Third-order Stokes interfacial waves for a density stratified two-layer fluid, Mem. Tokyo Met. Univ. 50 (2000) 120–136.
[32] J.B. Song, Generation of internal and surface waves by seafloor movement in a two layer fluid system, Theor. Comput. Fluid Dyn. 23 (2009) 197–211.
[33] E. Louis, J.A. Miralles, G. Chiappe, A. Bazán, J.P. Adrados, P. Cobo, Faraday instability in a vessel with a well: a numerical analysis, Phys. Fluid 23 (2011) 114102.